6th European Conference of the International Federation for Medical and Biological Engineering.
Vesely J, Horny L, Chlup H, Krajicek M, Zitny R, 2015. **The Influence of the Opening Angle on the Stress Distribution through the Saphenous Vein Wall**, IFMBE Proceedings Volume 45, 399-402. Manuscript version. Publisher link: http://link.springer.com/chapter/10.1007/978-3-319-11128-5_100

The Influence of the Opening Angle on the Stress Distribution through the Saphenous Vein Wall

J. Vesely[1], L. Horny[1], H. Chlup[1], M. Krajicek[2] and R. Zitny[3]

[1] Faculty of Mechanical Engineering Czech Technical University in Prague, Prague, Czech Republic
[2] First Faculty of Medicine, Charles University in Prague, Ruska 87, 100 00 Prague, Czech
[3] Faculty of Mechanical Engineering Czech Technical University in Prague, Prague, Czech Republic

Abstract—**In the present study, the inflation test of human *vena saphena magna* was conducted to obtain data suitable for multi-axial constitutive modeling at overloading conditions (pressures up to approximately 18 kPa). Subsequently the data were fitted with a hyperelastic, nonlinear and anisotropic constitutive model based on the theory of the closed thick-walled tube. It was observed that initial highly deformable behavior in the pressure–circumferential stretch response is followed by progressive large strain stiffening, which is in contrast to the pressure–axial stretch response. The effect of possible residual stress was evaluated in a simulation of the intramural stress distribution with the opening angle prescribed to 0°, 10°, 20°, 30°, 40°, and 50°. The result suggests that the optimal opening angle making the stress distribution through the wall thickness uniform is about 20°.**

Keywords— **bypass graft, inflation test, saphenous vein.**

I. Introduction

Autologous saphenous vein grafts are used in both coronary and peripheral bypass surgery as the gold standard [1, 2]. Their properties are, however, optimized for a mechanical environment very different from arterial conditions. Immediately after the surgery, remodeling processes are triggered and the vein adapts to the elevated blood pressure, flow rate and oscillatory wall shear stress [3]. As an undesirable effect of the changed conditions, the patency of the graft may be substantially compromised [4, 5].

Large attention has been paid to flow conditions and wall shear stress which are suspected to be responsible for intimal hyperplasia which frequently causes the graft failure (see e.g. [6, 7]). Varicose veins have been also studied from the mechanical and histological point of view [8, 9].

It has been known for decades that residual stresses/strains play significant role in blood vessels. The important influence of residual stresses, even of small magnitude, in arteries on the transmural stress distribution has been documented (e.g. [10]). It has been concluded that the consideration of residual stresses in physiological state leads to more homogenous circumferential stress through the thickness of the arterial wall, i.e. the stress gradient degreases (see e.g. [11, 12]).

The typical method to identify the residual strain in the blood vessel wall is the opening angle measurement [13]. The existence of residual stress is manifest by opening of an arterial ring when it is cut in the radial direction [14]. Therefore, the way how to incorporate the residual stresses is to consider an open sector of the cylindrical tube as the stress-free configuration. Here the opening angle is assumed to be constant along the axial direction [13].

The aim of this study was to identify the mechanical behavior of saphenous vein wall and to evaluate the residual strain effect on the stress distribution within the vein wall for venous and arterial conditions.

II. Material and Methods

A. Material

Human great saphenous vein for the inflation-extension test was collected during coronary-artery bypass surgery conducted at the General University Hospital in Prague (obtained with informed consent). The experimental protocol was approved by the Ethics Committee. Two rings were cut from the vein at both ends and the mean load-free geometry (external thickness and radius) of the sample was obtained from the photograph.

B. Theoretical framework

Kinematics: The vein was considered to be a homogeneous, incompressible cylindrical thick-walled tube. In cylindrical coordinates, let a material particle located at (R, Θ, Z) in the undeformed configuration be mapped to (r, θ, z) in the deformed vessel such that $r = r(R)$, $\theta = \pi/(\pi-\alpha)\ \Theta$, and $z = \lambda_z Z$.

When circumferential residual stress is taken into account through the opening angle α (Fig. 1), the circumferential stretch ratio becomes $\lambda_\theta = (\pi/(\pi-\alpha))r/R$. Here R is defined by equation (1). In (1) R_i is the inner radius of the unpressurized open vein [15].

$$R = \sqrt{\frac{\pi}{\pi-\alpha}\lambda_z\left(r^2 - r_i^2\right) + R_i^2} \quad (1)$$

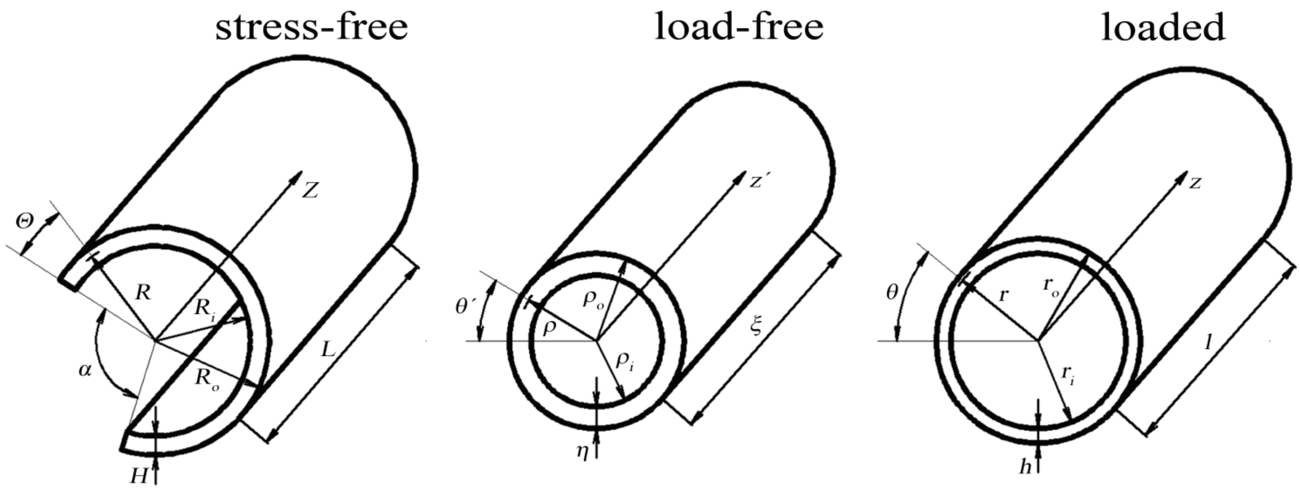

Fig. 1 Kinematics of the deformation with opening angle taken into account

Constitutive equations: The material of venous wall was considered to be an anisotropic hyperelastic continuum characterized by the strain energy density function W proposed by Holzapfel et al. [10]. The strain energy density function is expressed by equation (2).

$$W = \frac{\mu}{2}\left(I_1 - 3\right) + \frac{k_1}{k_2}\left(e^{k_2\left(I_4-1\right)^2} - 1\right) \qquad (2)$$

In (2) μ and k_1 are stress-like parameters, k_2 is dimensionless parameter. I_1 is the first invariant of the right Cauchy-Green strain tensor and I_4 is additional invariant arising from material anisotropy and has the meaning of square of the stretch in preferred (fiber) direction. I_1 and I_4 are defined in (3) and (4).

$$I_1 = \lambda_r^{\,2} + \lambda_\theta^{\,2} + \lambda_z^{\,2} \qquad (3)$$

$$I_4 = \lambda_\theta^{\,2}\cos^2\beta + \lambda_z^{\,2}\sin^2\beta \qquad (4)$$

In (4) β defines preferred direction within the material measured from circumferential axis of the tube in stress-free configuration of the vein.

Thick-walled tube: It can be demonstrated that the equilibrium equations relating the material response to the global loads with substituted constitutive equations are expressed via (5) and (6). Here $\hat{W}$ is the strain energy density function (2) with eliminated explicit dependence on λ_r substituting $\lambda_r = 1/(\lambda_\theta\lambda_z)$, P denotes internal pressure and F_{red} is the reduced axial force (prestretching) acting additionally to the force generated by the pressure pushing on the end of the tube [16], [17].

$$P = \int_{r_i}^{r_o} \lambda_\theta \frac{\partial \hat{W}}{\partial \lambda_\theta}\frac{dr}{r} \qquad (5)$$

$$F_{red} = \pi \int_{r_i}^{r_o}\left(2\lambda_z \frac{\partial \hat{W}}{\partial \lambda_z} - \lambda_\theta \frac{\partial \hat{W}}{\partial \lambda_\theta}\right) r\,dr \qquad (6)$$

Material parameters: The material parameters (μ, k_1, k_2, β) of the constitutive model were determined by fitting model predictions based on (5) and (6) to the experimental data for opening angle $\alpha = 0$. The objective function Q (7) was minimized in Maple 17. P^{mod} and P^{exp} in (7) denote the internal pressure predicted by (5) and measured experimentally, respectively. The same denotation applies for axial force F_{red}. Since the experiment was carried out in vertical position of the sample, $F_{red}^{\ exp}$ is given by the weight of the lover tube's plug (≈5g). Due to low weight, $F_{red}^{\ exp}$ was considered to be 0. w_p and w_F are weight factors.

$$Q = \sum_j \left\{\left[w_p\left(P_j^{mod} - P_j^{exp}\right)\right]^2 + \left[w_F\left(F_{redj}^{mod} - F_{redj}^{exp}\right)\right]^2\right\} \qquad (7)$$

Opening angle estimation: To provide qualified estimate of how large the residual strain in the venous wall could lead to the stress homogenization through the thickness, we computed the intramural distribution of the circumferential ($\sigma_{\theta\theta}$) and axial stress (σ_{zz}) defined in (8) for opening angles $\alpha = 0°$, $\alpha = 10°$, $\alpha = 20°$, $\alpha = 30°$, $\alpha = 40°$ and $\alpha = 50°$. Material parameters obtained in previous procedure were used in this simulation.

$$\sigma_{rr} = -\int_{r_i}^{r_o} \lambda_\theta \frac{\partial \hat{W}}{\partial \lambda_\theta} r\,dr \qquad \sigma_{ii} = \lambda_i \frac{\partial \hat{W}}{\partial \lambda_i} + \sigma_{rr} \qquad i = \theta, z \qquad (8)$$

C. Mechanical testing

The inflation-extension test was performed with the sample of the vein in order to obtain the experimental pressure-stretch data. The black marks were created on the surface of the specimen mounted in the experimental setup.

Four pre-cycles were carried out to stabilize the mechanical response, and a fifth cycle was used in the data analysis. The pressurization was performed in the range from 0 up to ≈18 kPa using a motorized syringe. The intraluminal pressure was recorded during the test by the pressure transducer (Cressto, Cressto s.r.o. Czech Republic). The sample was recorded by CCD camera (Dantec Dynamics, Skovlunde, Denmark) and the loaded configuration was evaluated using the edge detection method. The load-free geometry (Fig. 1) and the distance of longitudinal marks are listed in Table 1.

Table 1 The load-free geometry of the vein sample

Outer radius	ρ_o	2.89 mm
Thickness	η	0.83 mm
Distance of axial marks	ξ	11.20 mm

III. Results

A. Material parameters

Obtained material parameters are listed in Table 2. Fig. 2 shows the loading part of the fifth inflation-extension cycle to which the constitutive model was fitted. Model predictions were obtained by substituting the estimated parameters into the system (5) and (6).

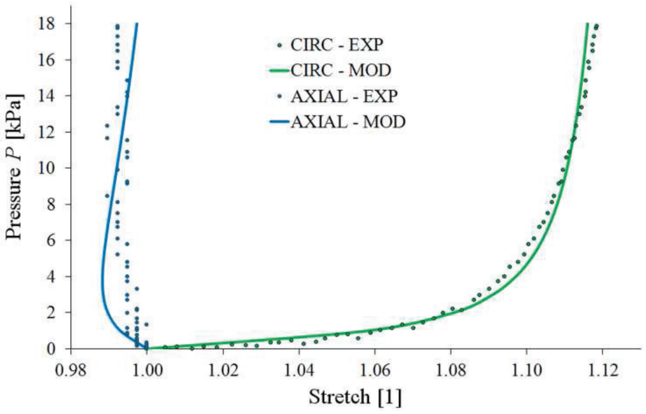

Fig. 2 Experimental (points) and model (solid line) pressure – stretch data for circumferential (CIRC) and axial (AXIAL) direction.

Table 2 Parameters of the constitutive model for the venous wall

μ [kPa]	k_1 [kPa]	k_2 [-]	β [rad]
13.04	0.24	60.30	0.75

B. Opening angle estimation

The influence of opening angle on the stress distribution through the vein wall for pressure P = 2.3 kPa (representative venous pressure) and P = 13.3 kPa (representative arterial pressure) are depicted in Fig. 3 with indicated numerical values of the intramural stress gradient, $\sigma_{kk}(r_i)/\sigma_{kk}(r_o)$ for $k = \theta, z$.

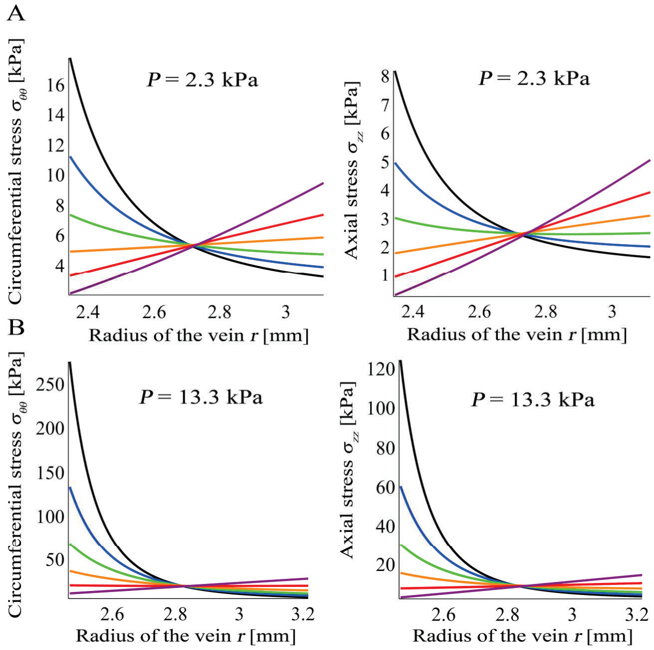

C

	$\alpha = 0°$	$\alpha = 10°$	$\alpha = 20°$	$\alpha = 30°$	$\alpha = 40°$	$\alpha = 50°$
$SR_\theta^{2.3kPa}$	5.60	2.91	1.56	0.84	0.44	0.21
$SR_z^{2.3kPa}$	5.03	2.47	1.22	0.57	0.23	0.05
$SR_\theta^{13.3kPa}$	42.38	16.15	6.37	2.56	1.02	0.39
$SR_z^{13.3kPa}$	38.25	14.38	5.51	2.09	0.73	0.19

Fig. 3 The simulation of the influence of opening angle α. The circumferential and axial stress gradients through the vein wall for transmural pressure 2.3 kPa (panel A) and for 13.3 kPa (panel B). Stress ratios at the inner and outer radius quantifying the stress gradient (panel C)

IV. Discussion and Conclusios

In our study, overloading inflation-extension test was performed on a sample of human saphenous vein. The experimental data was fitted by the hyperelastic nonlinear anisotropic constitutive model proposed by Holzapfel et al. [10]. Only the passive mechanical response was modeled.

Fig. 2 shows that the vein under simultaneous inflation and extension exhibit significantly smaller deformations in axial direction than in circumferential direction. This finding is in agreement with results of Wesly et al. [18], who studied the pressure-strain relationship of dog jugular and human saphenous veins.

We also tried to measure the residual strain by the opening angle method, but it was impossible with our current technical equipment. The vein wall was so compliant that it collapsed. The simulations of opening angle influence on the stress distribution suggest that the optimal opening angle (homogenizing the stress distribution across the wall thickness – uniform stress hypothesis; [11], [19]) could be expected to be from 20° to 30° for venous pressures.

The results also indicate that under arterial conditions the inner radius of the vein wall, which is originally optimized for low pressure, could be highly overloaded. This is consistent with the development of intimal hyperplasia after a graft surgery.

Acknowledgment

This study has been supported by Czech Ministry of Health grant no. NT 13302.

Conflict of Interest

The authors declare that they have no conflict of interest.

References

1. Perera GB, Mueller MP, Kubaska SM, Wilson SE, Lawrence PF, Fujitani RM (2004) Superiority of Autogenous Arteriovenous Hemodialysis Access: Maintenance of Function with Fewer Secondary Interventions. Ann Vas Surg 18:66-73.
2. Canver CC (1995) Conduit options in coronary artery bypass surgery. Chest 108:1150-1155.
3. Horny L, Chlup H, Zitny R, Konvickova S, Adamek T (2009) Constitutive behavior of coronary artery bypass graft, IFMBE Proc. vol. 25, World Congress on Med. Phys. & Biomed. Eng., Munich, Germany, 2009, pp 181–184
4. FitzGibbon GM, Kafka HP, Leach AJ, Keon WJ, Hooper GD, Burton JR (1996) Coronary bypass graft fate and patient outcome: Angiographic follow-up of 5,065 grafts related to survival and reoperation in 1,388 patients during 25 years. J Am Coll Cardiol 28:616-626
5. Hwang M, Berceli SA, Garbey M, Kim N H, Tran-Son-Tay R (2012) The dynamics of vein graft remodeling induced by hemodynamic forces: A mathematical model. Biomech Model Mechan 11:411-423
6. Tran-Son-Tay R, Hwang M, Garbey M et al. (2008) An experiment-based model of vein graft remodeling induced by shear stress. Ann Bimed Eng 36:1083-1091
7. Fernandez MC, Goldman DR, Jiang Z et al. (2004) Impact of shear stress on early vein graft remodeling: A biomechanical analysis. Ann Bimed Eng 32:1484-1493
8. Clarke GH, Vasdekis SN, Hobbs JT, Nicolaides AN (1992) Venous wall function in the pathogenesis of varicose veins. Surgery 111:402-408
9. Wali MA, Dewan M, Eid RA. (2003) Histopathological changes in the wall of varicose veins. Int Angiol 22:188-193
10. Holzapfel GA, Gasser TC, Ogden RW (2000) A new constitutive framework for arterial wall mechanics and a comparative study of material models. J Elast 61:1–48
11. Chuong CJ, Fung YC (1986) On residual stresses in arteries. J Biomech Eng 108:189-192
12. Fung YC (1991) What are the residual stresses doing in our blood vessels?, Ann Biomed Eng 19:237–249
13. Bustamante R, Holzapfel GA (2010) Methods to compute 3D residual stress distributions in hyperelastic tubes with application to arterial walls. Int J Eng Sci 48:1066–1082
14. Holzapfel GA, Sommer G, Auer M, Regitnig P, Ogden RW (2007) Layer-specific 3D residual deformations of human aortas with non-atherosclerotic intimal thickening. Ann Biomed Eng 35:530–545
15. Labrosse MR, Gersona ER, Veinot JP, Bellere CJ (2013) Mechanical characterization of human aortas from pressurization testing and a paradigm shift for circumferential residual stress. J Mech Behav Biomed 17:44-55
16. Horný L, Netušil M, Voňavková T (2013) Axial prestretch and circumferential distensibility in biomechanics of abdominal aorta. Biomech Model Mechan, in press
17. Matsumoto T, Hayashi K (1996) Stress and strain distribution in hypertensive and normotensive rat aorta considering residual strain. J Biomech Eng 118:62-71
18. Wesly RLR, Vaishnav RN, Fuchs JCA, Patel DJ, Greenfield JC Jr (1975) Static linear and nonlinear elastic properties of normal and arterialized venous tissue in dog and man. Circ Res 37:509-520
19. Takamizawa K, Hayashi K (1987) Strain energy density function and uniform strain hypothesis for arterial mechanics. J Biomech 20:7-17

Author: Jan Vesely
Institute: Czech Technical University in Prague
Street: Technicka 4
City: Prague 16607
Country: Czech Republic
Email: jan.vesely1@fs.cvut.cz